Activated carbons from biocollagenic wastes of the leather industry for mercury capture in oxy-combustion

M.A. Lopez-Anton*, R.R. Gil, E. Fuente, M. Díaz-Somoano, M.R. Martínez-Tarazona, B. Ruiz

Instituto Nacional del Carbón (CSIC), Francisco Pintado Fe, 26, 33011, Oviedo, Spain

*Corresponding author:

Phone: +34 985 119090
Fax: +34 985 297662
Email: marian@incar.csic.es

Abstract

This study evaluates the capacity of a series of activated carbons obtained from leather industry waste to retain mercury. The behaviour of these materials was compared in two simulated flue gas compositions at laboratory scale. The atmospheres were i) a typical coal oxy-fuel combustion atmosphere and ii) an O_2+N_2 atmosphere. The activated carbons displayed different behaviours depending on their characteristics and the gas composition. The best results were obtained for the activated carbon with the highest surface area and greatest amount of micropores, sulphur and acidity character, these results being comparable to those of an activated carbon impregnated with sulfur specifically designed for capturing elemental mercury. The highest level of mercury retention was achieved in a O_2+N_2 atmosphere. However, independently of the ability of these materials to capture mercury, their most interesting characteristic was their ability to oxidize mercury in an oxy-combustion atmosphere, since this would facilitate the retention of mercury in flue gas desulfurization units with the consequence that the risk of damage to the CO_2 compression and purification units would be reduced or even removed.

Keywords: mercury; activated carbons; biocollagenic wastes; leather industry; oxy-combustion

1. Introduction

Mercury and its compounds are highly toxic species which have a considerable impact on human health. Human activity has increased the mobilization of mercury species in the environment, raising the amounts in the atmosphere, soils, fresh waters, and oceans. Given the seriousness of these problems and the growing awareness about them, there is now global agreement on the need to reduce the emissions and release of mercury to the atmosphere. The Board of Directors of the United Nations Program for Environment (UNEP) in its Decision GC 25/5, created an Intergovernmental Negotiating Committee (INC) to develop a legally binding international agreement for mercury. Governments agreed to the text of a global legally binding instrument on mercury that was adopted in October 2013 [1]. The Treaty covers all aspects of the mercury life cycle, including anthropogenic mercury emissions to the air.

Anthropogenic sources of mercury emissions account for about 30% of the total amount of mercury entering the atmosphere each year [2]. The main industrial sources are coal combustion, metal production, the chlor-alcali industry, waste incineration, artisanal and small–scale gold mining and cement production [3]. In Europe 53.2% of the total amount of mercury emissions to the air recorded in 2010 came from coal combustion [4]. It must be remembered that mercury species are emitted to the air from industrial sources in three primary forms. One is gaseous elemental mercury (Hg^0), and all the other compounds in gas phase are grouped into what is called gaseous oxidized mercury (Hg^{2+}). The third group is mercury bound to particulates (Hg^p). In addition to the environmental problems caused by mercury species, mention should be made of the technological problems that Hg^0 may cause in oxy-combustion processes. Oxy-combustion is the combustion of fossil fuels in a highly oxygen-concentrated environment rather than air, as a result of which nitrogen is eliminated from the

combustion process. The result is a flue gas composed primarily of water and CO_2. The high concentration of CO_2 and absence of nitrogen in the flue gas simplify the separation of the CO_2 for storage or beneficial use. However, CO_2 compression and purification units can be damaged by Hg^0 due to the fact that this amalgamates with the aluminium of the heat exchangers [5-6].

Until now, the main solution for reducing mercury emissions has been to clean the gases produced from industrial sources by means of solid sorbents. In this way, mercury species are confined in a product that can be controlled. Various solid sorbents have been evaluated and used for the removal of inorganic mercury species in gas phase (Hg^0 and Hg^{2+}). They include non-carbon materials such as zeolites and calcium- and iron-based sorbents [7-9]. However, the most studied and commercialized sorbents for mercury capture have been activated carbons. Some activated carbons may be effective in capturing Hg^{2+} but in order to retain Hg^0 chemical impregnated sorbents are generally necessary [10-12]. A number of works in the literature describe the preparation and utilization of activated carbons for mercury removal, and some reviews have summarized this information [13-16]. In the search for high-quality sorbents different variables are taken into account, among which economic and environmental limitations need to be considered. This is the reason why some researchers have focused on the use of industrial or agricultural wastes as sorbents for mercury or as precursors for obtaining mercury sorbents [17-20]. The advantage of using this kind of material is not only the reduction in cost but also the environmental benefit gained from the revalorization of an industrial waste. In the search for a precursor for the preparation of activated carbons, solid wastes generated from the vegetable tanning of bovine skin in the Leather Industry (shavings, trimmings and buffing dust), were considered in this study. The leather waste mixtures (BCT) have low ash, high carbon and nitrogen contents and insignificant

amounts of metal species, making this material a highly suitable bioprecursor of activated carbons. Moreover, the use of BCT to obtain activated carbons provides a way to recover vegetable-tanned leather waste instead of disposal or incineration. A previous study using activated carbons derived from biocollagenic wastes from a vegetable tanning process demonstrated its high capacity for toluene adsorption compared to several commercial activated carbons [21].

The present research study aims to revalorise these types of biomaterials to obtain high added value activated carbons which can be used as adsorbent materials for different toxic elements, including mercury. Activated carbons with different physical and chemical characteristics were prepared to establish the main parameters that affect mercury retention. The behavior of these activated carbons for capturing mercury species was evaluated both in air and oxy-combustion atmospheres.

2. Experimental part

2.1. Materials

A leather waste blend was obtained by mixing and homogenising three types of solid bovine skin wastes; shavings, trimmings and buffing dust, from vegetable tanning. The blend was prepared by mixing each waste in the proportion in which it was generated in the Leather Industry; 84%, 15% and 1%, for shavings, trimmings and buffing dust, respectively. The total sample of the solid leather wastes (100 kg) was sampled for a period of one month being ground to <1 mm. A representative sample of 2 kg, obtained from the total sample, referred to as Biomaterial: Collagen & Tannins (BCT) was used as bioprecursor of the activated carbons.

Two methods were used to obtain the three activated carbons for mercury retention. The first method consisted in a two-stage process: i) carbonization of the raw material (BCT) to obtain a carbonized material or char (BCTP) and ii) chemical activation with KOH at a weight ratio of 1:1. This procedure gave the activated carbon labelled BCTP1. The second method consisted in the chemical activation of BCT with KOH at a weight ratio of 0.33:1 without the pyrolysis step. This activated carbon was labelled BCT0.33.

The precursor (BCT or BCTP) and the activating agent (KOH) were mixed in a solid state (physical mixture). After chemical activation the samples were washed to remove the activation products blocking the porosity. The samples were treated with a 5 mol dm^{-3} hydrochloric acid solution, rinsed with ultrapure water and dried at 105°C. A third activated carbon labelled BCTP1* was obtained from BCTP1 and washed at 100°C with hot water instead hydrochloric acid.

The mercury retention capacities were compared with that of a commercial activated carbon impregnated with sulphur (Norit RBHG3) specifically prepared for the capture of Hg^0.

2.2. *Experimental device for pyrolysis and activation experiments*

The experimental arrangement employed for the carbonization and activation of the precursor material has already been described in a previous work [22]. The pyrolysis and activation processes were carried out in an alumina crucible placed inside the tubular furnace under a 150 cm^3 min^{-1} flow of N_2 up to 750 °C, at a heating rate of 5 ºC min^{-1} for 1 h. The optimal conditions for the pyrolysis step were previously established [22]. About 10 g of BCT was used for the pyrolysis experiment and 5-10 g of BCT or BCTP and activating agent were used in the activation experiment.

2.3 Characterization of the raw materials and products

The moisture and ash contents of the sample were determined following the UNE 32002 and 32004 norms respectively, and the carbon, hydrogen, nitrogen and sulphur contents by means of automatic equipment. The concentration of chlorine was determined by means of an ion selective electrode.

The pH of the aqueous solutions obtained in every washing of the activated carbons were measured with a TIM870 Radiometer. The final conditions in the washing step were selected by controlling the pH until a constant value was obtained. The final pH value in the aqueous solutions is reflecting the chemical nature (acidity or basicity) in the activated carbons obtained.

The morphology of the samples was examined using a Scanning Electron Microscope equipped with an Energy-Dispersive X-Ray analysing system (SEM/EDX).

Textural characterization was performed by measuring the N_2 adsorption isotherms at -196°C. The isotherms were used to calculate the specific surface area S_{BET} and total pore volume, V_{TOT}, at a relative pressure of 0.95. The pore size distributions, microporosity and mesoporosity, were obtained by applying the density functional theory (DFT) model to the N_2 adsorption data, assuming slit-shaped pore geometry. Additionally, the narrow microporosity (pore width smaller than 0.7 nm) was estimated from CO_2 adsorption isotherms at 0°C using 1.023 g cm^{-3} as the density of adsorbed CO_2 and 0.36 as the b parameter. The CO_2 isotherms were used to calculate the micropore volume ($W_{0)}$, micropore size (L_0), energy characteristic (E_0) applying the Dubinnin-Raduskevich equation. In addition, the water vapour adsorption isotherms of the samples were determined at 25°C for water activity (aw) from 0 to 1. The equilibrium moisture content was expressed as grams per g of dry solid. The true

density of the materials was obtained by helium pycnometry. Before these experiments were performed the samples were outgassed under vacuum at 120°C overnight.

2.4 Experimental device for mercury retention experiments

The laboratory device used for retention of mercury is shown in Figure 1. The experimental device consists of a glass reactor heated by a furnace and fitted with a thermocouple. The sorbent bed was prepared by mixing 30 mg of activated carbon with 500 mg of sand. The elemental mercury in gas phase was obtained from a permeation tube and it was passed through the sorbent bed at 0.5 L min^{-1}. The concentration of mercury passed through the reactor was 100 $\mu g/m^3$. A synthetic gas mixture consisting of 4% O_2, 1000ppm SO_2, 1000ppm NO, 100 ppm NO_2, 25 ppm HCl, 12% H_2O, 64% CO_2 and 20% N_2 was employed as the simulated oxy-combustion atmosphere. The results were compared with those obtained in an O_2+N_2 atmosphere (12.6% O_2). The temperature of the sorbent and the gases was 150ºC. A continuous Hg emission monitor (VM 3000) was used to obtain the Hg adsorption curves. The mercury content after the retention experiments was determined by means of an automatic mercury analyzer (AMA). The duration of the mercury experiments was the time needed for the samples to reach maximum retention capacity.

The oxidation of mercury was evaluated by capturing the Hg^{2+} in an ion exchanger resin (Dowex® 1x8), specially designed for the selective extraction of Hg^{2+} species [23]. The resin was placed at the exit of the reactor prior to the Hg^0 continuous analyzer (Figure 1). The Hg^{2+} in the resin at the end of the retention experiments was determined by AMA. The resin had previously been conditioned with a mixture of HCl:H_2O (1:1) at 90ºC for 30 minutes and then filtered and dried.

The content of mercury condensate in the water and collected during the experiments prior to the analyzer was determined by AMA. The sulphate, nitrite and nitrate anion condensate in the water vapour was determined by ionic chromatography.

3. Results and discussion

3.1 Chemical characterization

Figure 2 shows the results of the chemical analysis corresponding to the mixture of the leather solid wastes (BCT), the carbonized material (BCTP), activated carbons (BCT0.33, BCTP1, BCTP1*) and the commercial activated carbon impregnated with sulphur (RBHG3). BCT has a low ash content (2.6%), and a high carbon and nitrogen contents (48.2 % and 7.5%, respectively) which makes this material a highly suitable bioprecursor for obtaining activated carbons. The pyrolysis step caused the thermal decomposition of the leather solid wastes with the subsequent elimination of volatile matter, producing a char, BCTP, with a higher carbon and ash content than BCT. These two materials, BCT y BCTP, were used as precursors of the activated carbons BCT0.33, BCTP1 and BCTP1* which have a carbon content of 81-91 % (Figure 2). The ash content is < 1.7 % for the materials that were washed with HCl (BCT0.33, BCTP1) whereas in the case of BCTP1* which was washed with hot water it is 10.5%. As is well-known, elements such as sulphur and chlorine may react with mercury and so these elements were also analysed in this study. BCT0.33 has the highest sulphur content (2%) of those adsorbent materials prepared from biocollagenic wastes obtained from the leather industry, although it is lower than that of RBHG3 (6%) (Figure 2). The chlorine content of both the BCT0.33 and BCTP1 activated carbons, which were washed with HCl, is approximately 0.03%. The pH values of BCT0.33 and BCTP1 are 3.6 and 4.1, respectively, whereas in the case of BCTP1* a basic pH of 10.4 was obtained.

3.2 Textural characterization and SEM-EDX

The N_2 adsorption isotherms at -196 ºC of the activated carbons used as mercury sorbents are shown in Figure 3. The adsorption of N_2 took place fundamentally at low relative pressures which is typical of microporous solids [24]. Moreover, the isotherms show a hysteresis loop, which is associated to capillary condensation inside the mesopores. Therefore the isotherms present a type I-IV hybrid shape, according to the BDDT classification [25]. The shape of the hysteresis loop is Type H4, according to the IUPAC nomenclature [24], which is often associated to narrow slit-like pores. The activated carbon obtained without a previous pyrolysis step (BCT0.33) presents the highest adsorption of nitrogen. Therefore, the pyrolysis step previous to the chemical activation does not seem to have contributed to the textural development of the activated carbon. Similar nitrogen adsorptions were obtained for the two carbonized activated carbons, adsorption being only slightly higher in the activated carbon washed with acid and water (BCTP1). These minor differences could be due to the high concentration of inorganic matter present in the activated carbon washed only with water (BCTP1*). The lowest nitrogen adsorption is corresponded to the commercial activated carbon RBHG3.

The results obtained with respect to the equivalent specific surface area S_{BET}, total pore volume V_{TOT} at a relative pressure of 0.95 and the pore size distributions (micropore and mesopores) by applying the density functional theory (DFT) model to the N_2 adsorption data for the activated carbons are presented in Table 1. The helium density of the materials is also shown in the Table 1 and as can be seen it is very similar for all the materials (~ 2.1 g cm^{-3}). BCT0.33 exhibited better results for S_{BET} and V_{TOT}, (1602 m^2g^{-1} and 0.695 cm^3g^{-1}, respectively) than the activated carbons subjected to

pyrolysis step prior to chemical activation. The lowest S_{BET} and V_{TOT} values (1078 m^2g^{-1} and 0.467 cm^3g^{-1}, respectively) correspond to BCTP1*. The commercial activated carbon presents a BET specific surface area of ~800 m^2/g.

An examination of the pore size distribution by means of the DFT method (Table 1 and Figure 3), revealed that the adsorbent materials obtained are essentially microporous (total micopore volume of up to 0.512 cm^3g^{-1}), with a low contribution of mesoporosity (total mesopore volume of up to 0.040 cm^3g^{-1}). Chemical activation of the original sample (BCT) resulted in BCT0.33 having a higher total micropore volume than the adsorbent material obtained by activation of BCTP due to the development of medium-sized microporosity. The pyrolysis step prior to chemical activation seems to have had a negative effect on the development of medium-sized microporosity (0.7-2 nm). However, the contribution of narrow microporosity (<0.7 nm) remained unchanged (Table 1).

The CO_2 adsorption isotherms at 0°C of the activated carbons are shown in Figure 4. In the case of porous carbons the adsorption of carbon dioxide at 0°C can be used to measure pore sizes, particularly in the case of ultramicroporosity (pores smaller than 0.7 nm). As can be seen from Figure 4, CO_2 uptake is similar for the activated carbons obtained from the leather wastes and in all cases higher than the CO_2 adsorption of RBHG3 over the entire relative pressure range. The micropore volume, W_0, energy characteristic (E_0) were calculated from the CO_2 isotherms by applying the Dubinnin-Raduskevich equation (Table 1). The activated material obtained from the leather residue, without the previous pyrolysis step, has a micropore volume (0.528 cm^3g^{-1}) which is higher than the values obtained from the carbonized leather residue (0.365 and 0.388 cm^3g^{-1}) (Table 1). As in the case of the N_2 isotherm, therefore the pyrolysis step prior to the chemical activation promotes the development of micropore volume to a

lesser extent. As for the average micropore size of the activated carbons (0.64-0.86) it is always slightly lower for the adsorbent materials obtained from the leather wastes by chemical activation with a previous pyrolysis step (Table 1).

Figure 5 shows the water vapour adsorption-desorption isotherms corresponding to the activated carbons. The water vapour adsorption isotherms are of type V also referred to as S-shaped [25] which is a consequence of the low interaction of the water molecules with the graphitic surface [26]. This type of isotherm is generally observed in microporous materials and often reported for activated carbons. The activated carbons obtained from the leather wastes present a higher adsorption than that of the commercial activated carbon. The isotherms show similar low adsorptions in the low relative pressure range but these increase dramatically from about $p/p^0 > 0.1$ in BCTP1 and BCTP1* and from $p/p^0 > 0.2$ in BCT0.33. The higher adsorption at the low relative pressure of BCTP1 and BCTP1* suggests a greater presence of surface functional groups, indicating that the pyrolysis step prior to the chemical activation increases the number of hydrophilic groups capable of forming hydrogen bonds with water molecules. The process of water adsorption is due to both to physical adsorption and chemical interaction with surface groups [26, 27]. Water molecules establish hydrogen bridges with the oxygen on the surface, in what are known as primary adsorption sites [26, 28], and subsequently water molecules will then bond with the previously adsorbed water molecules [26]. When this molecular cluster becomes sufficiently large, dispersion forces become predominant and it leaves the primary site to become adsorbed into hydrophobic micropores [29]. The isotherm shows a steep part (p/p= 0.3–0.7) associated with the steady growth of the water clusters. The region at a relative pressure higher than 0.7 is characterized by the high amount of water vapour adsorbed. The maximum adsorption is 0.557 g/g and 0.429 g/g in the case of BCT0.33 and

BCTP1 samples, respectively. Therefore, the material obtained by chemical activation without a previous pyrolysis step is more effective with respect to the total amount of water vapour adsorbed at the maximum p/p^0. The adsorption-desorption isotherms corresponding to the water vapour obtained show hysteresis loops, which are commonly attributed to pore filling and emptying mechanisms due to the condensation of water vapour in the pores of the activated carbon [30].

The SEM-EDX results (Figure 6) show the formation of macroporosity after chemical activation. It can be seen that the filamentous structure of the precursor has been destroyed after different chemical activations in all the samples. It can also be observed that the inorganic matter content of BCTP1* (Figure 6 c), visible in the form of small white brilliant fragments, is higher.

3.3 Mercury retention capacity

The mercury retention capacities and oxidation percentages of the activated carbons, in the O_2+N_2 and oxy-combustion atmospheres, are presented in Table 2. The confidence limit of the results is given as the standard deviation. Figures 7-8 show the mercury adsorption curves for the three activated carbons in the two atmospheres evaluated. As can be seen different mercury retention capacities were obtained depending not only on the characteristics of the activated carbons but also on the composition of the gases. The highest mercury retention was reached in the O_2+N_2 atmosphere with the activated carbon obtained from the leather residue following the procedure without a pyrolysis step (BCT0.33). The mercury retention capacity of BCT0.33 was of the order of that reached by the commercial activated carbon impregnated with sulphur (RBHG3). It must be borne in mind that the activated carbon BCT0.33 not only has the highest sulphur content but also the best textural

development. On the one hand, the presence of sulfur groups in the activated carbon BCT0.33 may facilitate the binding of Hg to the surface [12, 31] and on the other hand BCT0.33 has the highest S_{BET}, total pore volume and total micropore volume (Table 1) which may also favour mercury retention. It is well known that the Hg^0 adsorption mechanism occurs inside the micropores where the potential for interaction between the solid and the Hg^0 is significantly higher than in the wider pores [31]. The carbonized activated carbons (BCTP1, BCTP1*) show very different mercury retention capacities in the O_2+N_2 atmosphere (Figure 7), even though both carbons have similar textural characteristics. Two key differences between BCTP1 and BCTP1*, which would favour the mercury retention capacity in BCTP1 are: i) the presence of chlorine and ii) its acid character [32]. Therefore, for mercury retention in activated carbons, both a well-developed texture and the surface chemistry are important.

Especially remarkable are the huge differences in mercury behaviour between the O_2+N_2 atmosphere and the oxy-combustion atmosphere where O_2, CO_2 and H_2O vapour are present in major concentrations, and N_2, SO_2, HCl and NO_x in minor and trace concentrations. Apart from the characteristics of each activated carbon, a number of reactions between the gases (homogeneous oxidation) and interactions between the activated carbons and the gases (heterogeneous oxidation) must be taken into account to explain the different mercury retention capacities and speciations of each type of activated carbon.

The amount of mercury retained by the activated carbons (Table 2) is significantly lower in the oxy-combustion atmosphere (4% O_2, 1000ppm SO_2, 1000ppm NO, 100 ppm NO_2, 25 ppm HCl, 12% H_2O, 64% CO_2 and 20% N_2) than in the O_2+N_2 atmosphere. This conflicts with the hypothesis that the presence of SO_2/SO_3 in the gases has a beneficial effect. According to previous results by the authors and other

researchers [33-34] a higher proportion of oxidation of SO_2 to SO_3 occurs during oxy-combustion than in air combustion. After several investigations into the role of SO_2/SO_3 in mercury retention by activated carbons [35-39] it was concluded [12] that SO_3 in flue gases can cause the formation of H_2SO_4 on the activated carbon surface, which would enhance Hg^0 adsorption. However, in the present study SO_3 and/or H_2SO_4 might not be favoring Hg capture in the oxy-combustion atmosphere due to the slow kinetics of the reaction [12] where the activated carbon-gas contact time is lower than 1 second, similar to the contact time when activated carbon is injected into a coal-fired power plant. The reduction in mercury retention in oxy-combustion could be due to the adsorption of the CO_2 on the activated carbon. It must be remembered that in an oxy-combustion atmosphere CO_2 is present in concentrations of around 70-80%. CO_2 might be occupying part of the activated carbon microporous structure [31], in which case Hg and CO_2 would be competing for the same adsorption sites. In support of this hypothesis, the most marked decline in mercury retention was observed in the activated carbon with the highest micropore volume (BCT0.33) (Table 1).

The percentages of Hg^{2+} formed in both atmospheres are also very different. According to previous results by the authors, homogeneous oxidation of mercury occurs before the gas reaches the sorbent in an oxy-combustion atmosphere. Therefore, contrary to what occurs in an O_2+N_2 atmosphere where all the mercury that passes through the sorbent is in the form of Hg^0 ($Hg^{2+}(g)_{in}=0$), in oxy-combustion, approximately 30% of the Hg^0 is oxidized to Hg^{2+} ($Hg^{2+}(g)_{in}=30\%$) (Table 2). The main gases involved in this mercury oxidation would be SO_2, O_2 and NO [40-42] through the following reactions:

$$2Hg^0(g) + 2SO_2(g) + 2O_2(g) \rightarrow 2HgO(g) + 2SO_3(g) \qquad \text{fast} \qquad \text{(I)}$$

$$2\,Hg^0\,(g) + 2\,NO\,(g) \rightarrow 2\,HgO\,(g) + N_2\,(g) \qquad \text{very fast} \qquad (II)$$

Apart from homogeneous oxidation, reactions in aqueous phase produced by the condensation of a high amount of water vapor, which is typical of an oxy-combustion flue gas, may also occur. This would give rise to the formation of acid gases (reactions III, IV and V). Indeed, ion chromatographic analysis of the condensate water collected in a flask in the laboratory-scale device after the sorbent bed and prior to the elemental mercury analyzer (Figure 1), corroborated the presence of sulphates, nitrites and nitrates. The following reactions would then favor mercury oxidation through the formation of NO.

$$SO_3\,(aq,g) + H_2O\,(l,g) \rightarrow H_2SO_4\,(aq) \qquad \text{fast} \qquad (III)$$

$$2NO_2\,(g) + H_2O\,(l,g) \rightarrow HNO_2\,(aq) + HNO_3\,(aq) \qquad \text{slow} \qquad (IV)$$

$$3HNO_2\,(aq) \rightarrow HNO_3\,(aq) + 2NO\,(g) + H_2O\,(l,g) \qquad \text{fast} \qquad (V)$$

It is remarkable that the percentage of $Hg^{2+}(g)$ at the outlet of the sorbent bed ($Hg^{2+}(g)_{out}$), resulting from homogeneous and heterogeneous oxidation, increased to approximately 50-60% in BCT0.33 and in the commercial activated carbon (Table 2). The results suggests that the presence of reactive gases reduces the mercury retention capacity of the activated carbons but oxidizes Hg^0 to Hg^{2+}, especially in the case of those activated carbons with the highest mercury retention capacities, i.e. those with an acidic character, a higher surface area and greater micropores and sulphur content. The better textural development of BCT0.33 also implies a higher water adsorption at high pressures (Figure 5) which could favor the oxidation of mercury in an oxy-combustion atmosphere where high amounts of water vapor are present.

In addition to the formation of Hg^{2+} in gas phase, 20±5% of oxidized mercury was found in aqueous phase, i.e. Hg^{2+} analyzed in the condensate water collected prior to the mercury analyzer (Figure 1). The fact that a high proportion of Hg^0 oxidizes to Hg^{2+} in the presence of some of the activated carbons is very important considering that a cost-effective way to reduce mercury emissions during coal combustion processes would be to increase the oxidation of mercury to facilitate the capture of mercury in the flue gas desulphurization (FGD) units where Hg^{2+} can be retained. Moreover, as already mentioned, in the oxy-combustion process an increase in Hg^{2+} would be desirable as there would be less risk of damage to the CO_2 compression units.

4. Conclusions

Activated carbons obtained from leather industry waste are able to capture mercury in an O_2+N_2 atmosphere. High mercury retention capacities were achieved using an adsorbent material that was activated directly from the raw waste with KOH and washed with HCl and H_2O. In this case, the mercury retention capacity was of the order of that of a commercial activated carbon impregnated with sulphur. The pyrolysis step before activation resulted in the loss of surface area, micropores and sulphur, disfavouring mercury retention, whereas the acidic character of the activated carbons benefited the capture of mercury. The mercury retention capacity of the activated carbons decreased in an atmosphere of oxy-combustion but part of the Hg^0 was oxidized to Hg^{2+}. This behaviour could be exploited to retain mercury in FGD units already installed in power plants and to prevent the risk of damage to the CO_2 purification and compression units.

Acknowledgements

The authors acknowledge financial support by the National Research Program under the project CTM2011–22921. The authors thank Miquel Farrés Rojas S.A. for providing the leather wastes.

References

[1] United Nations Environment Programme (UNEP) http://www.unep.org/chemicalsandwaste/Mercury/Negotiations/tabid/3320/Default.aspx

[2] United Nations Environment Programme (UNEP) Global Mercury Assessment 2013: Sources, emissions, releases, and environmental transport, 42 pp, available in http://www.unep.org,

[3] United Nations Environment Programme (UNEP) Mercury: Time to act, 44pp, available in http://www.unep.org

[4] European Pollutant Release and Transfer Register http://prtr.ec.europa.eu

[5] Santos SO. Challenges in understanding the fate of mercury during oxyfuel combustion. IEA Greenhouse. Gas R&D Programme Cheltenham, United Kingdom. MEC7 Workshop DLCS, Strathclyde University, 18th June 2010

[6] Mitsui Y, Imada N, Kikkawa H, Katagawa A. Study of Hg and SO3 behavior in flue gas of oxy-fuel combustion system. Int J Green Gas Control 2011; 55:5143-50.

[7] Chojnacki A, Chojnacka K, Hoffmann J, Góreckia H. The application of natural zeolites for mercury removal: from laboratory tests to industrial scale. Miner Eng 2004; 17:933–7.

[8] Pavlish JH, Sondreal EA, Mann MD, Olson ES, Galbreath KC, Laudal D, Benson SA. Status Review of Mercury Control Options for Coal-fired Power Plants. Fuel Process Technol 2003; 82:89-165.

[9] Zhuang Y, Thompson JS, Zygarlicke CJ, Pavlish JH. Impact of Calcium Chloride Addition on Mercury Transformations and Control in Coal Flue Gas. Fuel 2007; 86:2351-9.

[10] Asasian N, Kaghazchi T. Optimization of activated carbon sulfurization to reach adsorbent with the highest capacity for mercury adsorption. Separ Sci Technol 2013; 48:2059-72.

[11] His H-C, Chen C-T. Influences of acidic/oxidizing gases on elemental mercury adsorption equilibrium and kinetics of sulphur-impregnated activated carbon. Fuel 2012; 98:229-35.

[12] Morris EA, Kirk DW, Jia CQ. Roles of sulphuric acid in elemental mercury removal by activated carbon and sulphur-impregnated activated carbon. Environ Sci Technol 2012; 46:7905-12.

[13] Sjostrom S, Durham M, Bustard CJ, Martin C. Activated carbon injection for mercury control: Overview. Fuel 2010; 89:1320-2.

[14] López-Antón MA, Tascón JMD, Martínez-Tarazona MR. Retention of mercury in activated carbons in coal combustion and gasification flue gases. Fuel Process Technol 2002; 77-78:353-8.

[15] Lee SH, Park YO. Gas-phase mercury removal by carbon-based sorbents. Fuel Process Technol 2003; 84:197-206.

[16] Reddy KSK, Shoaibi AA, Srinivasakannan C. Elemental mercury adsorption on sulphur-impregnated porous carbon-A review. Environ Technol 2014; 35:18-26.

[17] Skodras G, Diamantopoulou I, Zabaniotou A, Stavropoulos G, Sakellaropoulos GP. Enhanced mercury adsorption in activated carbons from biomass materials and waste tires. Fuel Process Technol 2007; 88:749-58.

[18] Tan Z, Qiu J, Zeng H, Liu H, Xiang J. Removal of elemental mercury by bamboo charcoal impregnated with H_2O_2. Fuel 2011; 90:1471-5.

[19] Asasian N, Kaghazchi T, Soleimani M. Elimination of mercury by adsorption onto activated carbon prepared from the biomass material. J Ind Eng Chem 2012; 18:283-9.

[20] Klasson KT, Lima IM, Boihem Jr LL, Wartelle LH. Feasibility of mercury removal from simulated flue gas by activated chars made from poultry manures. J Environ Manage 2010; 91:2466-70.

[21] Gil RR, Ruiz B, Lozano MS, Martín MJ, Fuente E. VOCs removal by adsorption onto activated carbons from biocollagenic wastes of vegetable tanning. Chem Eng J 2014; 245:80–8.

[22] Gil RR, Girón RP, Lozano MS, Ruiz B, Fuente E. Pyrolysis of biocollagenic wastes of vegetable tanning. Optimization and kinetic study. J Anal Appl Pyrol 2012; 98:129-36.

[23] Fuente-Cuesta A, Díaz-Somoano M, López-Antón MA, Martínez-Tarazona MR. Oxidised mercury determination from combustion gases using an ionic exchanger. Fuel 2014; 122:218-22.

[24] Sing KSW, Everett DH, Haul RAW, Moscou L, Pierotti RA, Roquerol J, Siemieniewska T. Reporting physisorption data for gas/solid systems. Pure Appl Phys Chem 1985; 57:603-19.

[25] Brunauer S, Deming LS, Deming WE, Teller E. On a theory of the van der Waals adsorption of gases. J Am Chem Soc 1940; 62:1723-32.

[26] Dubinin MM. Water vapor adsorption and the microporous structures of carbonaceous adsorbents. Carbon 1980; 18:355-64.

[27] Foley NJ, Thomas KM, Forshaw PL, Stanton D, Norman PR. Kinetics of water vapor adsorption on activated carbon. Langmuir 1997;13:2083-9.

[28] Dubinin MM, Zaverina ED, Serpinsky VV. The sorption of water vapour by active carbon. J Chem Soc 1955; 1760-6.

[29] Do DD, Do HD. A model for water adsorption in activated carbon. Carbon 2000; 38:767-73.

[30] Lagorsse S, Campo MC, Magalhaes FD. Mendes A. Water adsorption on carbon molecular sieve membranes: Experimental data and isotherm model. Carbon 2005; 43:2769-79.

[31] Diamantopoulou I, Skodras G, Sakellaropoulos GP. Sorption of mercury by activated carbon in the presence of flue gas components. Fuel Process Technol 2010; 91:158-63.

[32] Fuente-Cuesta A, Díaz-Somoano M, López-Antón MA, Cieplik M, Fierro JLG, Martínez-Tarazona MR. Biomass gasification chars for mercury capture from a simulated flue gas of coal combustion. J Environ Manage 2012; 98:23-8.

[33] Stanger R, Wall T. Sulphur impacts during pulverized coal combustion in oxy-fuel technology for carbon capture and storage. Prog Energ Combust 2011; 37:69-88.

[34] Koornneef J, Ramirez A, van Harmelen T, van Horssen A, Turkenburg W, Faaij A. The impact of CO2 capture in the power and heat sector on the emission of SO2, NOx, particulate matter, volatile organic compounds and NH3 in the European Union. Atmos Environ 2010; 44:1369-85.

[35] Zhuang Y, Martin C, Pavlish J, Botha F. Cobenefit of SO3 reduction on mercury capture with activated carbon in coal flue gas. Fuel 2011; 90:2998-3006.

[36] Presto AA, Granite EJ. Impact of sulfur oxides on mercury capture by activated carbon. Environ Sci Technol 2007; 41:6579-84.

[37] Granite EJ, Presto AA. Comment on the role of SO2 for elemental mercury removal from coal combustion flue gas by activated carbon. Energ Fuel 2008; 22:3557-8.

[38] Uddin MdA, Yamaha T, Ochiati R, Sasaoka E, Wu S. Role of SO2 for elemental mercury removal from coal combustion flue gas by activated carbon. Energ Fuel 2008; 22:2284-9.

[39] Morris EA, Morita K, Jia CQ. Understanding the effects of sulfur on mercury capture from coal-fired utility flue gases. J Sulfur Chem 2010; 31:457-75.

[40] Fuente-Cuesta A, López-Antón MA, Díaz-Somoano M, Martínez-Tarazona MR. Retention of mercury by low-cost sorbents: Influence of flue gas composition and fly ash occurrence. Chem Eng J 2012; 213:16-21.

[41] Rodríguez-Pérez J, López-Antón MA, Díaz-Somoano M, García R, Martínez-Tarazona MR. Regenerable sorbents for mercury capture in simulated coal combustion flue gas. J Hazard Mater 2013; 260:869-77.

[42] Abad-Valle P, López-Antón MA, Díaz-Somoano M, Martínez-Tarazona MR. The role of unburned carbon concentrates from fly ashes in the oxidation and retention of mercury. Chem Eng J 2011; 174:86-92.

Table 1. Textural properties of the activated carbons

Sample	ρHe g cm^{-3}	S_{BET} m^2 g^{-1}	V_{TOT} $cm^3 g^{-1}$	V um[a] cm^3 g^{-1}	V mm[a] cm^3 g^{-1}	V_{tot} microp[a] cm^3 g^{-1}	V mesop[a] cm^3 g^{-1}	W_0 cm^3 g^{-1}	E_0 KJ/mol	L nm
			p/p^0=0.95	< 0.7 nm	0.7-2 nm	< 2 nm	2 - 50 nm			
BCT0.33	2.12	1602	0.695	0.249	0.264	0.512	0.021	0.528	23.92	0.86
BCTP1	2.05	1163	0.506	0.249	0.126	0.374	0.040	0.365	27.16	0.69
BCTP1*	2.12	1078	0.467	0.238	0.105	0.343	0.019	0.388	28.18	0.64

[a] Evaluated from DFT applied to N_2 adsoption isotherm at – 196 ºC.

Table 2. Capacities of mercury retention and percentages of homogeneous and heterogeneous oxidation for the activated carbons in a O_2+N_2 and an oxy-combustion atmosphere.

Sample	**O_2+N_2**			**Oxy-combustion**		
	Hg ret. ($\mu g\ g^{-1}$)	$Hg^{2+}(g)_{in}$ (%)	$Hg^{2+}(g)_{out}$ (%)	Hg ret. ($\mu g\ g^{-1}$)	$Hg^{2+}(g)_{in}$ (%)	$Hg^{2+}(g)_{out}$ (%)
BCT0.33	2007±200	0	0	160±15	33±6	60±6
BCTP1	822±100	0	0	24.2±3	31±5	32±5
BCTP1*	127±5	0	1	9.1±2	25±5	23±5
RBHG3	1649±200	0	1	127±10	32±5	50±5

Hg ret.: mercury retention capacity; $Hg^{2+}(g)_{in}$: oxidized mercury by homogeneous oxidation; $Hg^{2+}(g)_{out}$: oxidized mercury by homogeneous and heterogeneous oxidation

Figure captions

Figure 1. Schematic diagram of the experimental device used for mercury retention

Figure 2. Chemical composition of the materials

Figure 3. N_2 adsorption isotherms at -196 ºC and pore size distribution applying the DFT method to the activated carbons.

Figure 4. CO_2 adsorption isotherms at 0ºC of the activated carbons

Figure 5. Water vapour adsorption isotherms at 25ºC of the activated carbons

Figure 6. SEM micrographs of the activated carbons (x5000): a) BCT0.33; b) BCTP1; c) BCTP1*.

Figure 7. Mercury adsorption curves obtained for the activated carbons in a O_2+N_2 atmosphere

Figure 8. Mercury adsorption curves obtained for the activated carbons in an oxy-combustion atmosphere

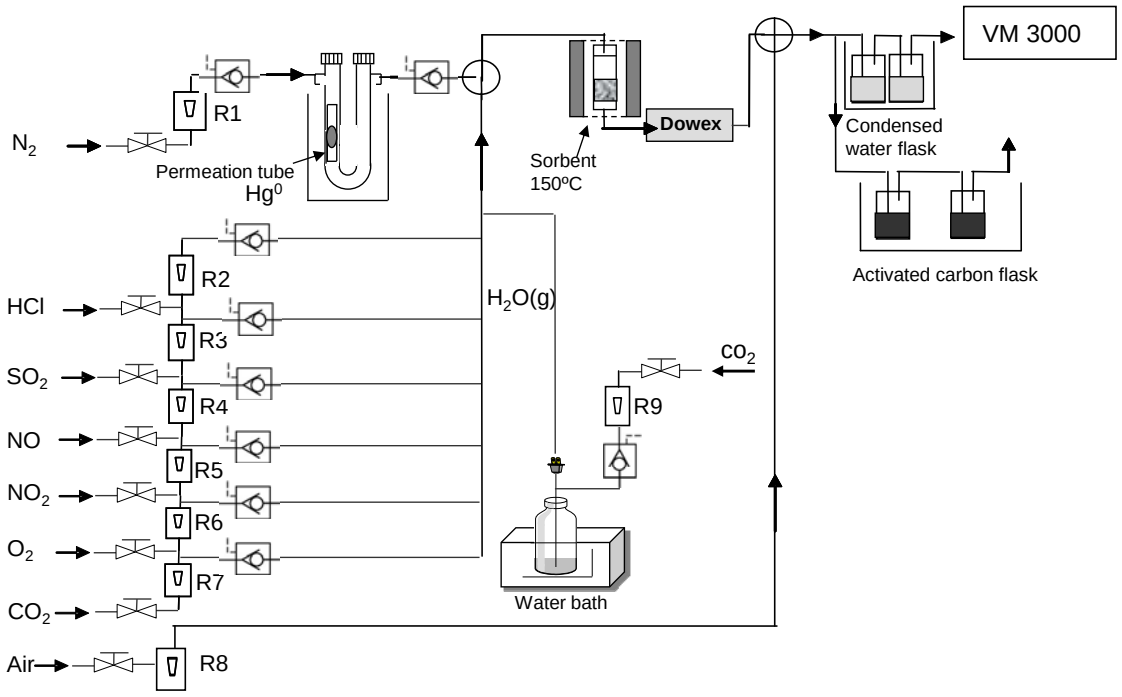
VM 3000
R1
N2
Permeation tube
Hg0
Sorbent
150ºC
Dowex
Condensed
water flask
Activated carbon flask
R2
HCl
R3
SO2
R4
NO
R5
NO2
R6
O2
R7
CO2
Air
R8
H2O(g)
CO2
R9
Water bath

Figure 1.

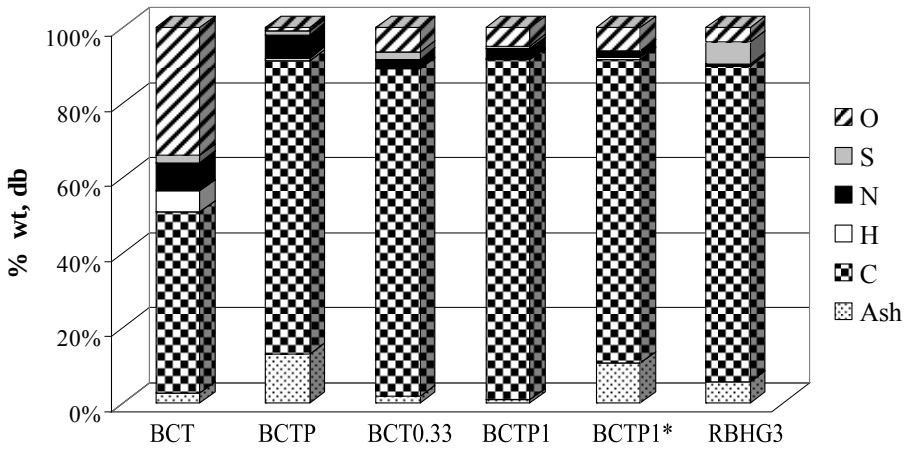
100%
80%
60%
40%
20%
0%
% wt, db
BCT
BCTP
BCT0.33
BCTP1
BCTP1*
RBHG3
O
S
N
H
C
Ash

Figure 2.

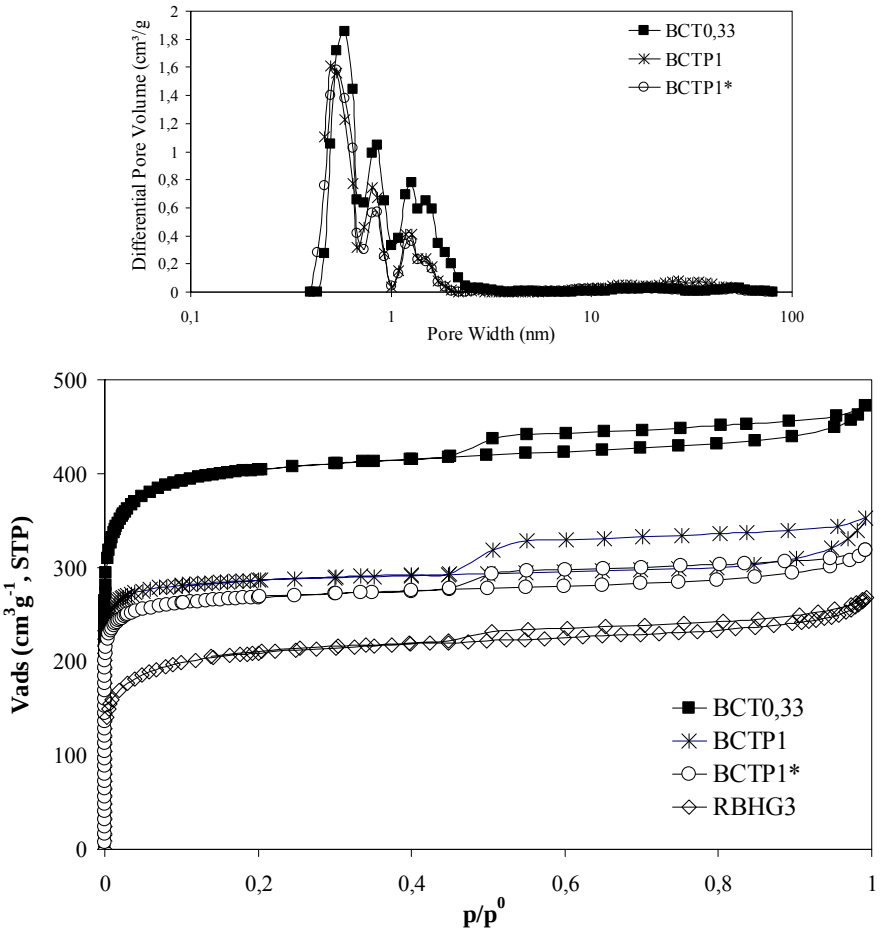
Differential Pore Volume (cm³/g
Pore Width (nm)
BCT0,33
BCTP1
BCTP1*
Vads (cm³g⁻¹, STP)
p/p⁰
BCT0,33
BCTP1
BCTP1*
RBHG3

Figure 3.

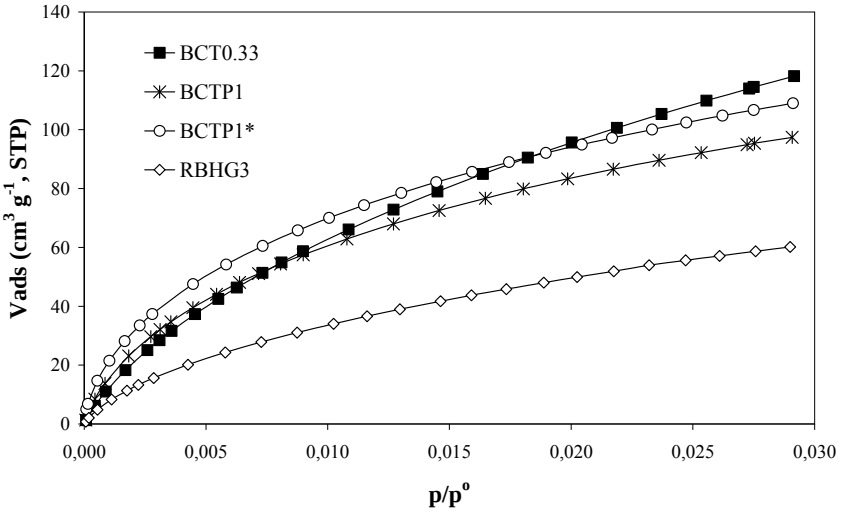
BCT0.33
BCTP1
BCTP1*
RBHG3
Vads (cm3 g-1, STP)
p/p°
140
120
100
80
60
40
20
0
0,000
0,005
0,010
0,015
0,020
0,025
0,030

Figure 4.

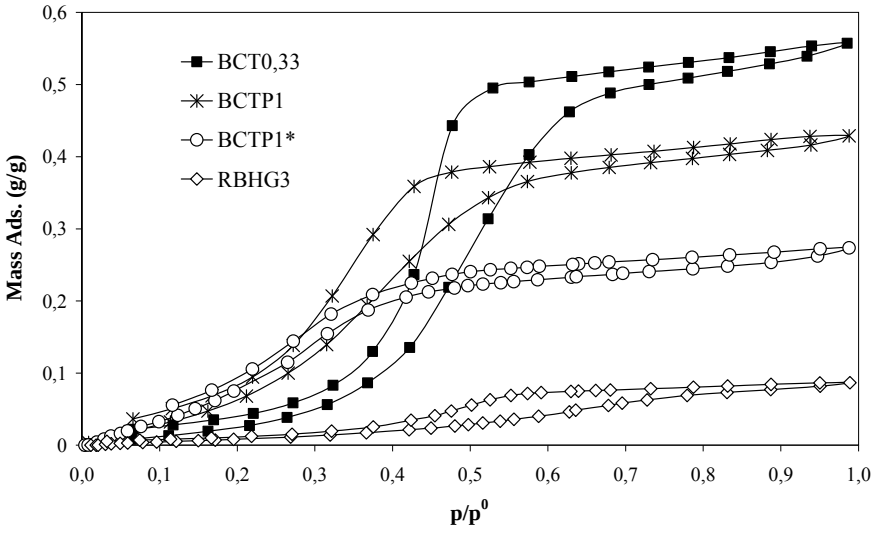
0,6
0,5
0,4
0,3
0,2
0,1
0
Mass Ads. (g/g)
BCT0,33
BCTP1
BCTP1*
RBHG3
0,0
0,1
0,2
0,3
0,4
0,5
0,6
0,7
0,8
0,9
1,0
p/p0

Figure 5.

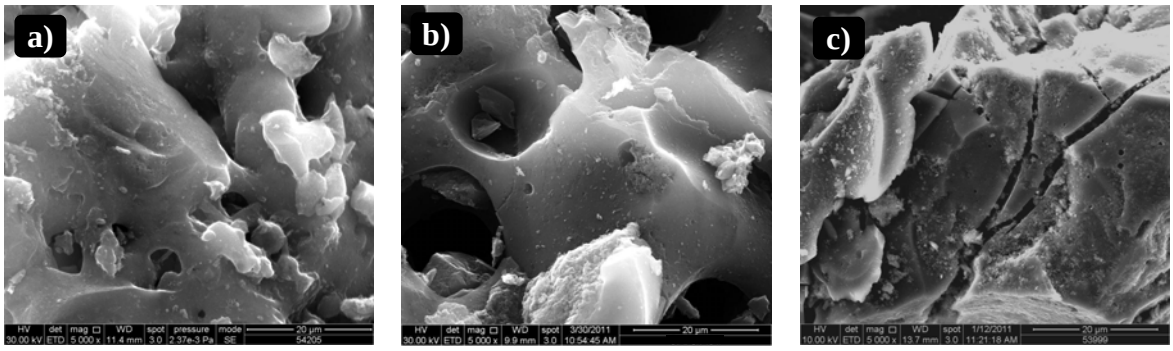

Figure 6